Automatic Brain Image Segmentation for Evaluation of Experimental Ischemic Stroke Using Gradient Vector Flow and Kernel Annealing

Umut Ozertem[1]*, Andras Gruber*[2]*, and Deniz Erdogmus*[1,2]
Departments of [1]CSEE and [2]BME, Oregon Health and Science University, Portland, Oregon, USA

ABSTRACT

Ischemic stroke is the most prevalent catastrophic disease of the brain. Various animal models have been used to study the disease. The majority of the models are based on induction of focal ischemic cerebral necrosis, followed by exhaustive morphometric analysis of the tissues. Despite recent advances in machine learning and image processing, neurological damage evaluations are still based on tedious manual or semi-automatic segmentation of brain images. We demonstrate a method that uses active contours combined with a kernel annealing approach to automatically segment the brain organs of interest, as well as a simple feature that highlights the contrast between normal and infarct brain tissue for automated analysis. The automated segmentation and analysis solution will be useful for increasing the productivity of experimentation and removing investigator bias from the data analysis.

1. INTRODUCTION

Stroke research is often performed in small animal models, including rodents. The ischemic stroke is usually induced experimentally, and the effect or benefits of various interventions, including new drugs, are evaluated. The process requires sophisticated and reliable imaging and analysis of the neurological damage in the affected hemisphere of the brain. The results of these experiments help identify new molecular targets for better treatment or prevention of stroke. Brain image analysis in experimental stroke has been performed either manually or semi-automatically by using basic image processing tools [1-3]. In brief, in most rodent experiments, ischemic stroke is induced by temporal or permanent occlusion of one of the middle cerebral arteries. Part of the brain that does not receive sufficient blood supply develops an ischemic infarct (necrosis) within hours to days. Once the brain is removed, it can be sliced into standard size segments, and the necrotic region, usually visible on the affected side of the brain, can be visualized with a special stain. The infarcts then can be quantified (e.g., in percentage of ipsilateral or contralateral area, or in volume) using morphometric analysis. Automatic image segmentation of the brain, certain organs of interest in the brain, and the infarct region will enable fast, accurate and reliable analysis of the desired statistics by removing investigator bias from the data analysis.

Earlier image segmentation methods are based on thresholding the edge-map of the image to build the segment contours [4]; however, these methods are applicable only if the intensity values contain sufficient information. More recent methods include split and merge approaches and region-based approaches, which have the advantage of low computational cost, but suffer from the sensitivity to design parameters, which may lead to unstable solutions [5,6]. Nonparametric clustering based approaches can be employed to circumvent these difficulties; however, the success of this approach relies on the construction of features that will lead to perceptually relevant and important clusters [7]. A relatively recent proposal that improves upon the edge-map technique is the use of active contours (snakes) [8]. Original snakes suffer from low capture range with respect to a particular initialization, and poor convergence towards boundary concavities [9]. Mainly due to the low capture range problem the use of snakes for image segmentation is very limited, and if it is not initialized close to the *true boundary*, the snake is likely to converge to a wrong solution. To provide the required good initialization for snakes, in some applications, rather than using it as the segmentation algorithm by itself, snakes are only used in the postprocessing of another segmentation algorithm as a fine-tuning step.

Gradient vector flow formulation overcomes these drawbacks by introducing another class of external forces for active contours [9]. As long as the majority of the contour that defines the boundary is detected by the edge detection step, even coarse initializations will lead to good segmentation results for images with relatively constant foreground and background. But still, in cases where either the foreground or the background –or maybe both- has a texture with high variations, the edges resulting from texture might attract the active contour. This presents a significant challenge for the particular brain image segmentation problem we aim to solve. Especially, the neurologically damaged portion of the brain has a sharply varying texture. In general, we have observed that fine-tuning the parameters of the snakes to identify the desired segments properly (assessed by visual inspection) is a daunting task. This is still true in the gradient vector field formulation, where an additional parameter controls the trade-off between robustness and suboptimality for noisy or highly textured images. More significantly, the interval

of parameter values that provide the *visually-almost-optimal result* may vary for each particular image (different slices of the same brain).

Our goal is to develop an automated brain image analysis system for rigorous neurological studies of the brain to assess the effects of ischemic strokes. The final solution is envisioned to utilize atlas-based brain-organ boundary initialization followed by active contour based organ segmentation and feature/clustering-based infarct classification. To this end, this paper contributes the following: (1) we incorporate a deterministic kernel annealing procedure to increase the robustness of gradient vector flow based active contours for brain segmentation, (2) we propose a simple feature that improves the contrast between the infarct and healthy regions, enabling accurate clustering based segmentation of these two types of tissue.

2. PARAMETRIC SNAKE MODEL AND CONVOLUTION SMOOTHING

The parametric snake model was originally proposed by Kass and colleagues [8] and revisited by Xu and Prince [9]. A two dimensional snake $\mathbf{c}(s)=[x(s),y(s)]$ is a closed contour parameterized by the parameter s varying between 0 and 1. For a particular image, the optimal snake is the curve that minimizes the following energy functional:

$$E = \int_0^1 \left[\alpha \left|\mathbf{c}'(s)\right|^2 + \beta \left|\mathbf{c}''(s)\right|^2 \right] + E_{ext}(\mathbf{c}(s))\, ds \quad . \tag{1}$$

In this formulation α, and β define the weights to adjust the *tension* and the *rigidity* of the snake, where these values are defined as the magnitude-squared integral of the first and second derivatives of the snake with respect to s. Hence, the first two terms in (1) define the internal energy function. The externally defined part of the energy function, E_{ext}, is determined by the image features. A proper E_{ext} takes smaller values at the boundaries of segments. For binary images (pixels intensities are 0 or 1), a suitable external energy functions is $E_{ext} = G(x,y) * I(x,y)$, where $G(x,y)$ is a Gaussian function that is introduced to eliminate some local minima and to increase the capture range [8]. Distance potential forces are also introduced as an alternative way to improve the capture range [10], however, these do not address the problem of concavities. For grayscale images, a typical energy function is the negative magnitude of the spatial gradient of intensities. The smoothened energy functional is $E_{ext} = -\left\|G(x,y) * \nabla I(x,y)\right\|^2$ [8].

By manipulating the width of the kernel (window size for rectangular kernels, standard deviation for Gaussian kernels), one can control the amount of smoothing in order to overcome the low capture range difficulty around boundaries. Wider kernels will remove small fluctuations in E_{ext} by blurring the force field and the boundaries, thus will increase the capture range increases.

The optimizer of the objective function in (1) should satisfy the following Euler equation

$$2\alpha\, \mathbf{c}''(s) - 2\beta\, \mathbf{c}^{(4)}(s) - \nabla E_{ext} = 0 \tag{2}$$

which can be rewritten as a force balance equation as reorganizing the forces resulting from the internal and external energy functions. Explicitly,

$$F_{ext} = -\nabla E_{ext} \qquad F_{\text{int}} = 2\alpha\, \mathbf{c}''(s) - 2\beta\, \mathbf{c}^{(4)}(s) \tag{3}$$

and the resulting balance equation is $F_{\text{int}} + F_{ext} = 0$. The solution to (3) is obtained by a iterating a suitable fixed point algorithm:

$$\mathbf{c}_{n+1}(s) = 2\alpha\, \mathbf{c}_n''(s) - 2\beta\, \mathbf{c}_n^{(4)}(s) - \nabla E_{ext} \ . \tag{4}$$

3. GRADIENT VECTOR FLOW

Gradient vector flow (GVF) addresses the low capture range issue and solves the concavity problem at the same time [8,9]. A static external *gradient vector field* $\mathbf{v}(x,y)$ is defined. Replacing $-\nabla E_{ext}$ with $\mathbf{v}(x,y)$ yields $2\alpha\mathbf{c}''(s) - 2\beta\mathbf{c}^{(4)}(s) - \mathbf{v} = 0$.

Clearly, as desired, $\mathbf{v}$ takes its larger values at the boundaries, since it is built on a feature map $f(x,y)$ that has larger values at the object boundaries, but $\mathbf{v}$ is not necessarily maximized exactly at the edges. Nevertheless, the induced suboptimality effect is weaker than kernel smoothing that would provide the same capture range. A natural $f(x,y)$ is $-\nabla E_{ext}$ for any suitable E_{ext} of choice. For any given f, $\mathbf{v}(x,y)=[u(x,y), v(x,y)]$ is the minimizer of

$$S = \iint \left(\mu \left(\|u\|^2 + \|v\|^2\right) + \left|\nabla f\right|^2 \left|\mathbf{v} - \nabla f\right|^2 \right) dx\, dy \tag{5}$$

The criterion in (5) is designed to reduce problematic features of f while preserving its desirable qualities, with the parameter μ controlling the trade-off [9].

The GVF formulation diminishes two major problems present in the original snakes, but still the technique is susceptible for noisy or textured images. It also suffers from sensitivity to parameter selections – specifically for the brain images we have, the intervals of parameter values that yield proper results are quite narrow.

4. KERNEL AND THRESHOLD ANNEALING

The method we propose is based on the GVF technique where the optimal vector field $\mathbf{v}$ is determined for a smoothened and thresholded Canny edge-map of the original image. Specifically, we let

$$f(x,y) = UnitStep\left(\left\| K_\sigma(x,y) * E_{canny}(x,y) \right\|^2 - T \right) \tag{6}$$

where E_{canny} is the binary Canny edge map of the image, T is the annealed edge-detection threshold, and K_σ is a suitable smoothing kernel.[1] The kernel size is annealed logarithmically and the threshold is annealed linearly. The force field $\mathbf{v}$ is calculated from (5) at each annealing step.

[1] $K_\sigma(x,y) \ge 0$, $\iint K_\sigma(x,y)dxdy = 1$, and $\lim_{\sigma\to 0} K_\sigma(x,y) = \delta(x,y)$.

When these annealing procedures are incorporated into the calculation of the force fields: (i) annealing of the threshold helps to initially eliminate spurious edges (these might include some portions of the actual target boundary), while asymptotically all significant edges are recovered; (ii) annealing of the kernel size helps to initially avoid local minima but asymptotically approach the global minimum of the original energy functional as determined from the low-threshold edge map given by (2). The proposed annealing procedure is motivated by the well known theory of smoothing functionals in global optimization [11], and our previous experience with kernel annealing for global optimization of nonlinear systems [12]. Feature space annealing has been established as a method for seeking robust solutions in noisy feature spaces [13]. The algorithm is summarized in Table 1.

Table 1. Summary of the proposed algorithm

1. Determine the binary Canny edge map E_{canny} for the image (or use any binary/continuous edge detector).
2. Start annealing loop by setting a large kernel size σ and a large threshold T.
   - *i*) Determine f using (6)
   - *ii*) Determine $\mathbf{v}$ by minimizing (5)
   - *iii*) Iterate the snake $\mathbf{c}$ using (4) and $\mathbf{v} = \nabla E_{ext}$
   - *iv*) Anneal σ and T, go to (*i*), if stopping criterion reached, stop.

5. AUTOMATIC BRAIN IMAGE SEGMENTATION AND NEUROLOGICAL DAMAGE DETECTION

We are particularly focusing on the automated segmentation of brain images acquired through a microscope-camera system that generates high-resolution photographs of the brain laid on grid-paper, where the grids are used for pixel-length conversions to calculate volumes. The automation will enable a more accurate (less bias and variance) neurological damage assessment due to ischemic strokes in rodents. The main organ of interest is the cortex. Specifically, in this paper, we will focus on:

(i) finding the brain boundary in the image,
(ii) finding the cortex boundary in the brain,
(iii) determining the infarct region

The first two are achieved by adapting two snakes initialized manually to the vicinity of the desired objects; the brain snake is initialized as an ellipse that contains the brain, and the cortex snake is initialized as an ellipse contained in the cortex, based on visual inspection of the images. The third problem is solved by determining a discriminative feature that emphasizes the separation between healthy and infarct portions. Specifically, a feature map $g(x,y)$ is evaluated for each pixel coordinate (x,y) as the root-mean-squared intensity in a square neighborhood centered around the pixel as follows:

$$m(x,y) = \frac{1}{(2L+1)^2} \sum_{i=-L}^{L} \sum_{j=-L}^{L} I(x-i, y-j)$$

$$s^2(x,y) = \frac{1}{(2L+1)^2} \sum_{i=-L}^{L} \sum_{j=-L}^{L} (I(x-i, y-j) - m(x-i, y-j))^2 \quad (7)$$

$$g(x,y) = m(x,y) + s(x,y)$$

The neighborhood size we used is L=5. Once this feature is extracted for each pixel, any clustering algorithm (or classification algorithm if labeled training data is available) can be utilized. The feature given in (7) has worked successfully in clustering the infarcts and healthy portions on the images available to us using simple thresholding. The results for brain and cortex segmentation as well as infarct classification are shown in Fig 1 for two sample slices (from front and back) from our image database.

6. CONCLUSIONS

Ischemic stroke is the most prevalent catastrophic disease of the brain. Affects of this disease on the brain is studied by inducing stroke in small rodents, imaging the extracted and sliced brain under a microscope, and manually analyzing the images to quantify the amount of neurological damage to the affected hemisphere. The automation of this image analysis procedure would benefit the basic scientific research in this important field by eliminating human bias and variance and increasing the speed of analysis, while reducing workload and dependency on trained analysts (who undergo months of supervised training to come to an acceptable level).

In this paper, we presented an active contour based segmentation approach to identify the brain and internal organs. The active contours are trained in an annealing loop in order to achieve global optimization. To classify the damaged portion of the brain, a simple feature is derived based on visual inspection and it is shown to achieve high classification accuracy through simple threshold based clustering.

Future work will (*i*) incorporate atlas-based initialization of active contours to segment the brain and the organs of interest, (*ii*) three-dimensional deformable image registration between segmented brain slices and internal organs to determine proper 3-D segmentation of the volumetric regions, (*iii*) investigate other useful features that will help discriminate neurologically damaged tissue from healthy tissue (*iv*) incorporate expert-labeled data to achieve supervised classification of these tissues. Based on our experiences with the current images, we are also planning to improve the image acquisition setup in order to facilitate the segmentation procedure using active contours and classification techniques. Modifications will include realigning the light source and the camera to minimize shadow effects, using a better quality microscope and a color camera combination, and blank background to eliminate the unnecessary challenge resulting from the grids.

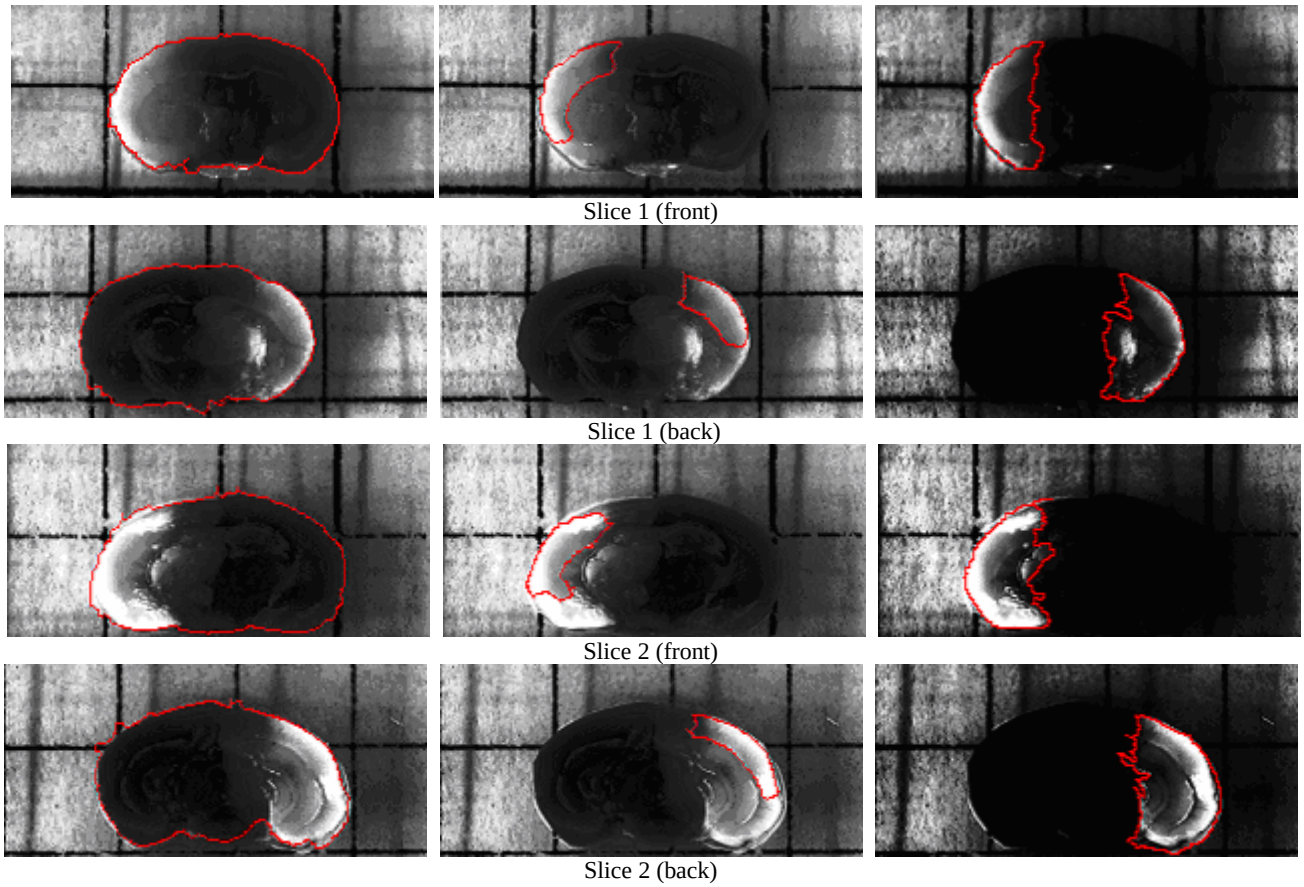

Figure 1. The contours obtained for the brain (left), cortex (middle) and the damaged portion (right) for two brain slices each for top and bottom view.

6. ACKNOWLEDGEMENTS

The authors would like to thank Sawan Hurst for performing the stroke experiments and preparing the brain specimens, and to Xubo Song and Misha Pavel for valuable discussions. This work is partially supported by the NSF grants ECS-0524835, and ECS-0622239.

7. REFERENCES

[1] M. Shibata, S.R. Kumar, A. Amar, J.A. Fernandez, F. Hofman, J.H. Griffin, B.V. Zlokovic, "Anti-inflammatory, Antithrombotic, and Neuroprotective Effects of Activated Protein C in a Murine Model of Focal Ischemic Stroke," Circulation, vol. 13, pp. 1799-1805, 2001.

[2] H. Offner, S. Subramanian, S.M. Parker, M.E. Afentoulis, A.A. Vandenbark, P.D. Hurn, "Experimental Stroke Induces Massive, Rapid Activation of the Peripheral Immune System," Journal of Cerebral Blood Flow and Metabolism, 2005. [E-publication ahead of print]

[3] T.F. Choudhri, B.L. Hoh, C.J. Prestigiacomo, J. Huang, L.J. Kim, A. M. Schmidt, W. Kisiel, E.S. Connolly Jr, D. J. Pinsky, "Targeted Inhibition of Intrinsic Coagulation Limits Cerebral Injury in Stroke without Increasing Intracerebral Hemorrhage," J Exp Med, vol. 1, pp. 91-99, 1999.

[4] J.F. Canny, "A Computational Approach to Edge Detection," IEEE Transactions on Pattern Analysis and Machine Intelligence, vol. 8, pp. 679-698, 1986.

[5] R. Pal, S.K. Pal, "A Review in Image Segmentation Techniques," Pattern Recognition, vol. 26, pp.1277-1294, 1993.

[6] K.S. Fu, J.K. Mei, "A Survey on Image Segmentation," Pattern Recognition, vol. 13, pp. 3-16, 1981.

[7] K. Fukunaga, L.D. Hostetler, "The Estimation of the Gradient of a Density Function, with Applications in Pattern Recognition," IEEE Transactions on Information Theory, vol. 21, pp. 3240, 1975.

[8] M. Kass, A. Witkin, D. Terzopoulos, "Snakes: Active Contour Models," International Journal of Computer Vision, vol.1, pp. 321-331, 1987.

[9] C. Xu, J.L. Prince, "Snakes, Shapes, and Gradient Vector Flow," IEEE Transactions on Image Processing, vol. 7, pp. 359-369, 1998.

[10] L.D. Cohen, I. Cohen, "Finite-Element Methods for Active Contour Models and Balloons for 2-D and 3-D Images," IEEE Pattern Analysis and Machine Intelligence, vol. 15, pp. 1131-1147, 1993.

[11] R.Y. Rubinstein, /Simulation and the Monte Carlo Method/, John Wiley & Sons, New York, 1981.

[12] D. Erdogmus, J.C. Principe, "Generalized Information Potential Criterion for Adaptive System Training," vol. 13, pp. 1035-1044, 2002.

[13] K. Rose, "Deterministic Annealing for Clustering, Compression, Classification, Regression and Related Optimization Problems," Proceedings of IEEE, vol. 11, pp. 2210-2239, 1998.